Polarforschung 64 (2): 75–88, 1994 (erschienen 1995)

Subglacial and Seabed Topography, Ice Thickness and Water Column Thickness in the Vicinity of Filchner-Ronne-Schelfeis, Antarctica.

By D.G. Vaughan[1], J. Sievers[2], C.S.M. Doake[1], H. Hinze[3], D.R. Mantripp[4], V.S. Pozdeev[5], H. Sandhäger[6], H.W. Schenke[3], A. Solheim[7] and F. Thyssen[6]

Summary: Modelling of the deformation and evolution of the Antarctic Ice Sheet, and the oceanographic conditions on the continental shelf around Antarctica, requires good datasets that accurately describe the environment. We present thematic maps of subglacial and seabed topography, and water column thickness, over Filchner-Ronne-Schelfeis, its hinterland and the adjacent portion of Weddell Sea. Subglacial and seabed topography were derived from various bathymetric observations, seismic and radar soundings. Ice shelf draft was deduced from an inversion of ERS-1 radar altimetry, assuming hydrostatic equilibrium. Finally, the water column thickness was calculated as the difference between the sea bed depth and the ice shelf draft.

The seabed morphology beneath the ice shelf is dominated by a slope down towards the interior of the continent. Seabed depths near the ice front of around 200 to 300 m increase to more than 1500 m at the grounding line of some ice streams. Deep troughs, possibly glacially deepened, run beneath the eastern and western sides of the ice shelf and cross the continental shelf. An area of small water column thickness to the north-west of Berkner Island suggests that extensive grounding could occur after a relatively small change in the ice shelf. This might result in very significant changes to the positions of the Berkner Island summits and the rates of production of Ice Shelf Water (ISW).

Zusammenfassung: Für die Modellierung der Entwicklung und Veränderung des Eises der Antarktis sowie der ozeanographischen Randbedingungen auf dem antarktischen Kontinentalschelf bedarf es umfassender geowissenschaftlicher Datensätze, welche die Umwelt hinreichend genau beschreiben. Hierzu werden vom Filchner-Ronne-Schelfeis, seinem Hinterland und dem angrenzenden Bereich der Weddell Sea die Topographie des Meeresbodens und des Eisuntergrunds sowie die Schelfeismächtigkeit und die Höhe der Wassersäule unter dem Schelfeis als thematische Karten vorgestellt. Die Topographie des Meeresbodens und des Eisuntergrundes wurden aus bathymetrischen, seismischen und Radarmessungen verschiedener Kampagnen abgeleitet. Die Mächtigkeit des Schelfeises wurde aus der Umkehrung von ERS-1-Radaraltimetermessungen hergeleitet, wobei ein hydrostatisches Gleichgewicht des schwimmenden Eises angenommen wurde. Schließlich wurde die Höhe der Wassersäule als Differenz zwischen der Meerestiefe und der Schelfeismächtigkeit berechnet.

Die Morphologie des Meeresbodens unter dem Schelfeis wird durch eine Abwärtsneigung dominiert, die zum Inneren des Kontinents gerichtet ist. Meerestiefen, die in der Nähe der Eisfront 200 bis 300 m betragen, vergrößern sich auf über 1500 m an der Aufsetzlinie einiger Eisströme. Tiefe Tröge, wahrscheinlich von Gletschern ausgehöhlt, verlaufen unterhalb der östlichen und der westlichen Seite des Schelfeises und durchqueren den Kontinentalschelf. Ein Gebiet mit geringer Mächtigkeit der Wassersäule im Nordwesten von Berkner Island legt die Vermutung nahe, daß hier schon bei relativ geringen Änderungen des Fließverhaltens und der Dicke des Schelfeises ausgedehnte Auflagerungen eintreten können. Als Folgeerscheinung kann es dann sowohl zu starken Veränderungen bei der Lage der Gipfel auf Berkner Island als auch bei der Entstehung von Schelfeiswasser unter dem Schelfeis kommen.

[1] David G. Vaughan and Christopher S.M. Doake, British Antarctic Survey, Madingley Road, Cambridge, CB3 OET, United Kingdom.

[2] Jörn Sievers, Institut für Angewandte Geodäsie, Richard-Strauss-Allee 11, D-60598 Frankfurt am Main, Germany.

[3] Heinrich Hinze and Hans-Werner Schenke, Alfred Wegener Institute for Polar and Marine Research, P.O. Box 12 01 61, D-27515 Bremerhaven, Germany.

[4] David R. Mantripp, Mullard Space Science Laboratories, Holmbury St. Mary, Dorking, RH5 6NT, United Kingdom.

[5] Vitaly S. Pozdeev, Polar Marine Geology Expedition, Sevmorgeologija, Pobeda St. 24, 188510 St. Petersburg, Russia.

[6] Henner Sandhäger and Franz Thyssen, Forschungsstelle für physikalische Glaziologie, Westfälische Wilhelms-Unversität Münster, Corrensstrasse 24, D-48149 Münster, Germany.

[7] Anders Solheim, Norsk Polarinstitutt, Middelthunsgate 29, P.O. Box 5072 Majorstua, N-0301, Oslo, Norway.

Manuscript received 28 February 1995; accepted 10 July 1995

1 INTRODUCTION

Antarctic ice shelves play an important role in the global climate system. Their influence pervades much of the Antarctic Ice Sheet and, through the interactions with the ocean, a considerable fraction of the Earth's surface. Long term trends and shifts in global climate can only be understood by examining both the atmospheric and the oceanographic circulation patterns and the major controls on these processes; ice shelves are one such control.

The two largest ice shelves, Ross Ice Shelf and Filchner-Ronne-Schelfeis (FRS) (Fig. 1) have been the focus of considerable research effort. Using the most recent compilation of Antarctica maps, Fox & Cooper (1994) recalculated the area of the floating portions of the Ross Ice Shelf (494,213 km^2) and FRS (449,220 km^2). Being significantly thicker than Ross Ice Shelf, FRS is the most massive body of floating ice in the world today. Indeed, ice flowing into FRS accounts for around 15 % of the total accumulation on the grounded ice sheet of Antarctica, excluding the Antarctic Peninsula (240 Gt a^{-1}, Giovinetto & Bentley 1985).

Two mechanisms in particular transmit the influence of FRS worldwide. Firstly, changes in size of the grounded ice sheet nourishing FRS are reflected immediately in global sea level. The West Antarctic Ice Sheet (WAIS) is a marine ice sheet, grounded on rock that is below sea level, and its discharge is determined, to a significant degree, by the glaciers and ice streams that flow into FRS.

Secondly, modification of the sea water beneath FRS influences the circulation pattern in the oceans. Around 70 % of the oceanographic water mass known as Antarctic Bottom Water (AABW) is produced in the Weddell Sea region (Carmack 1990). AABW is a cold dense body of water that is a product of deep convection in the Southern Ocean (Farbach et al. 1994). It has a characteristically high density and so spreads through the deep ocean as far as 53° N (Mantyla & Reid 1983), and

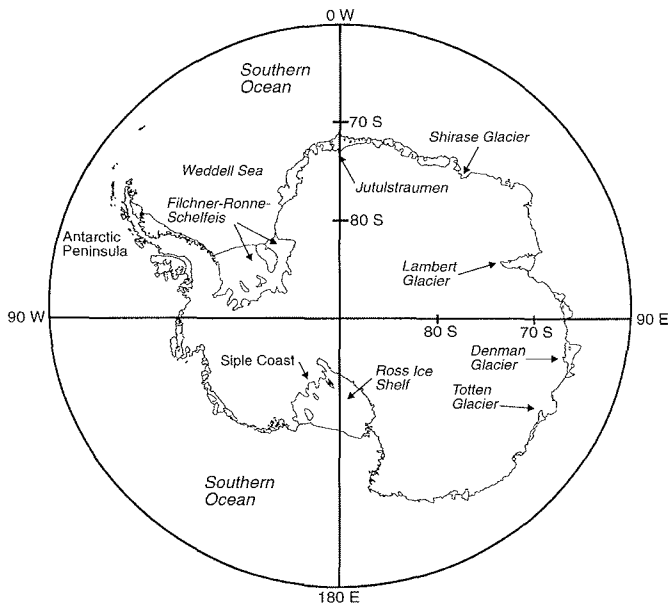

Fig. 1: Antarctic location map.

Abb. 1: Lagekarte der Antarktis.

since it is also oxygen-rich, both ventilates and cools the oceans. In the Weddell Sea AABW forms from mixing between Weddell Sea Bottom Water (WSBW) and Deep Water (DW) in the Weddell Gyre. One mechanism for the production of WSBW relies on the ice shelf base being exposed to circulating sea water and forming an intermediate water, Ice Shelf Water (ISW) (FOLDVIK & GAMMELSRØD 1988). Production of ISW might be drastically reduced if a change in the ice shelf thickness caused a different pattern of grounding, closing off the present routes of access, reducing the area of the sub-ice shelf cavity ventilated by ocean currents and resulting in a reduction of the production of AABW. This could well be manifested in a large scale alteration of vertical transport in the Southern Ocean.

Clearly, there are strong imperatives for understanding the past, and predicting the future, behaviour of ice shelves such as FRS. Simple models of ice sheets and ice shelves that use idealised, or grossly smoothed geometry are inadequate to predict the particular behaviour of the real ice sheet resting on a highly complex topography. In real ice sheets even small features may have a profound influence (DOAKE & VAUGHAN 1991). Plausible attempts to predict the future behaviour of the ice sheet/ice shelf/ ocean system by prognostic mathematical modelling rely heavily on the availability of high quality maps of the current ice and bedrock.

In this paper we describe the preparation and implications of a new thematic map published by VAUGHAN et al. (1994; see Appendix) showing subglacial and seabed topography beneath FRS, its hinterland and the adjacent Weddell Sea as well as the oceanographic water column beneath the ice shelf.

We refer to the entire ice shelf, as *Filchner-Ronne-Schelfeis* (FRS) and to the subdivisions east and west of Berkner Island as *Filchnerschelfeis* and *Ronne Ice Shelf* respectively. This is done without implication, but following the relevant provisions of the Antarctic Treaty.

2 MAP OF SUBGLACIAL AND SEABED TOPOGRAPHY

The aim of the project was to use the best available data to map the elevation of the seabed in the open sea and under the ice shelf, as well as the elevation of the ice/rock interface beneath the grounded ice sheet. In such environments, the different overlying materials present differing obstacles to observation of the rock surface. The optimum method depends on the environment, so data from a variety of techniques were used. In the open sea we chose shipborne sonar, on the ice shelf seismic reflection data and airborne radar sounding with barometric altimetry on the grounded ice. Original data from published sources were used along with unpublished data from the participating institutes. During preparation of the map the area was divided into zones (Appendix-sources diagram). The sources of data used in the compilation are described in detail in Appendix - explanatory text. A schematic map of the distribution of the data is shown in Figure 2.

The data were contoured in three separate areas; a) Zone A: the southern Weddell Sea, using methods described by HINZE (1994); b) Zone D: Berkner Island, using methods described by SANDHÄGER (1993); c) The remainder, FRS and its hinterland. Data were assembled and processed using a geographic information system. Additional constraints were imposed at grounding lines and over ice rumples where the ice thickness could be estimated with confidence from radar sounding data. The gridding used linear interpolation of the triangulated data onto a regular grid, from which contours were drawn automatically. The resulting contours were smoothed by hand to produce the final map (Appendix - main map). The seabed topography is shown using black contour lines and block colours. The subglacial topography is shown using brown contour lines only but is overlaid with visible satellite imagery to allow comparison of surface features with subglacial topography.

Although we have chosen to present bedrock contours beneath all of the ice shelf, paucity of data in Zone H means that bedrock elevation in this area is speculative. The contouring presented honours the available data at the boundary of this zone but is subjective within.

3 WATER COLUMN THICKNESS MAP

The water column thickness map shown (Appendix - inset diagram) is constructed by subtracting the bedrock elevation grid from a coincident grid representing the ice shelf draft. Ice shelf thickness and draft was derived by applying a hydrostatic equilibrium relation to a grid of ice shelf surface elevation (SIEVERS et al. 1995; Fig. 3). A further constraint was imposed at the

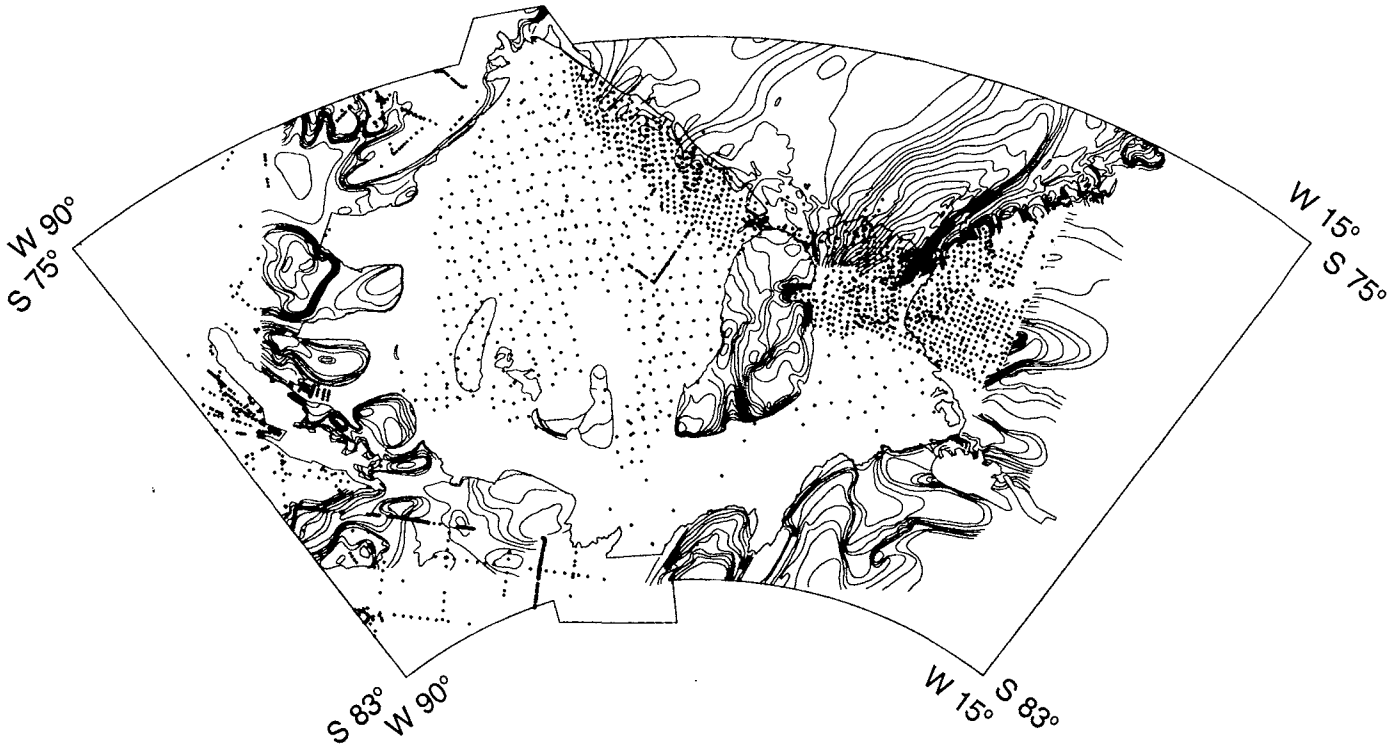

Fig. 2: Distribution of subglacial and seabed elevation data used in the compilation beneath Filchner-Ronne-Schelfeis and in the hinterland.

Abb. 2: Lage der Meßpunkte und Profile, die zur Ableitung der Topographie des Meeresbodens und des Eisuntergrundes unter dem Filchner-Ronne-Schelfeis und in seinem Hinterland verwendet wurden.

grounding lines, where the water column thickness is necessarily zero.

Filchner-Schelfeis front underwent a substantial change in 1986 with the calving of icebergs A22, A23 and A24 (FERRIGNO & GOULD 1987). Ronne Ice Shelf front has undergone several less significant events. To be compatible with the ERS-1 data, acquired in 1992, we have used an ice front for this period which is different from that shown by SWITHINBANK et al. (1988).

There are still large areas beneath FRS for which there have been few measurements of bedrock elevation and these contribute directly to uncertainty in the water column map. In the present compilation we have attempted to make reasonable guesses of the bedrock elevation in these areas, and note the need to collect more data.

Calculating the ice shelf draft

FRS is formed from two types of ice: *meteoric ice,* comprising ice draining from the inland ice sheet and ice accumulated on the surface of the ice shelf itself, comprising direct snow-fall, redistributed snow and hoar frost; and *marine ice,* frozen directly to the base of the ice shelf as a layer underlying the meteoric ice, in areas controlled by oceanographic conditions (ROBIN et al. 1983, ENGELHARDT & DETERMANN 1987, THYSSEN 1988, OERTER et al. 1992). The body of marine ice beneath the central region of Ronne Ice Shelf is notable because it is vast in area (THYSSEN et al. 1993) and thickness (up to 400 m). Its mechanism of formation is also unusual (BOMBOSCH & JENKINS 1995), giving rise to an unusual composition, structure and properties (OERTER et al. 1992). The high-frequency conductivity of marine ice is significantly higher than that for meteoric ice, giving an impedance contrast at the meteoric/marine ice interface which produces a strong radar reflection. Furthermore, since the marine ice is considerably more lossy to radio-waves, absorption usually prevents the marine ice/ocean interface from being observed. Maps of ice thickness measurements based on radar sounding (ROBIN et al. 1983, CRABTREE & DOAKE 1986, THYSSEN 1988, THYSSEN et al. 1993) were thus interpreted as showing only meteoric ice thickness. ROBIN et al. (1983) mapped the approximate areal distribution of marine ice by interpreting the strength of the return from the base of the meteoric ice.

The presence of marine ice means that radar sounding is inadequate for mapping total ice thickness over the areas with marine ice, but additionally, radar sounding fails elsewhere. Areas that show surface, basal or intermediate crevassing (THYSSEN et al. 1993) rarely give satisfactory radar echoes, as voids and density changes within the ice act as scattering centres, cluttering the radar return and obscuring the true basal echo.

Seismic sounding is more reliable since the density contrast between meteoric and marine ice is low, and this interface gives a weak reflection. The marine ice/ocean interface is more reflective, and also the marine ice is not particularly lossy to seismic energy. In most areas the ice/ocean interface is resolvable. There

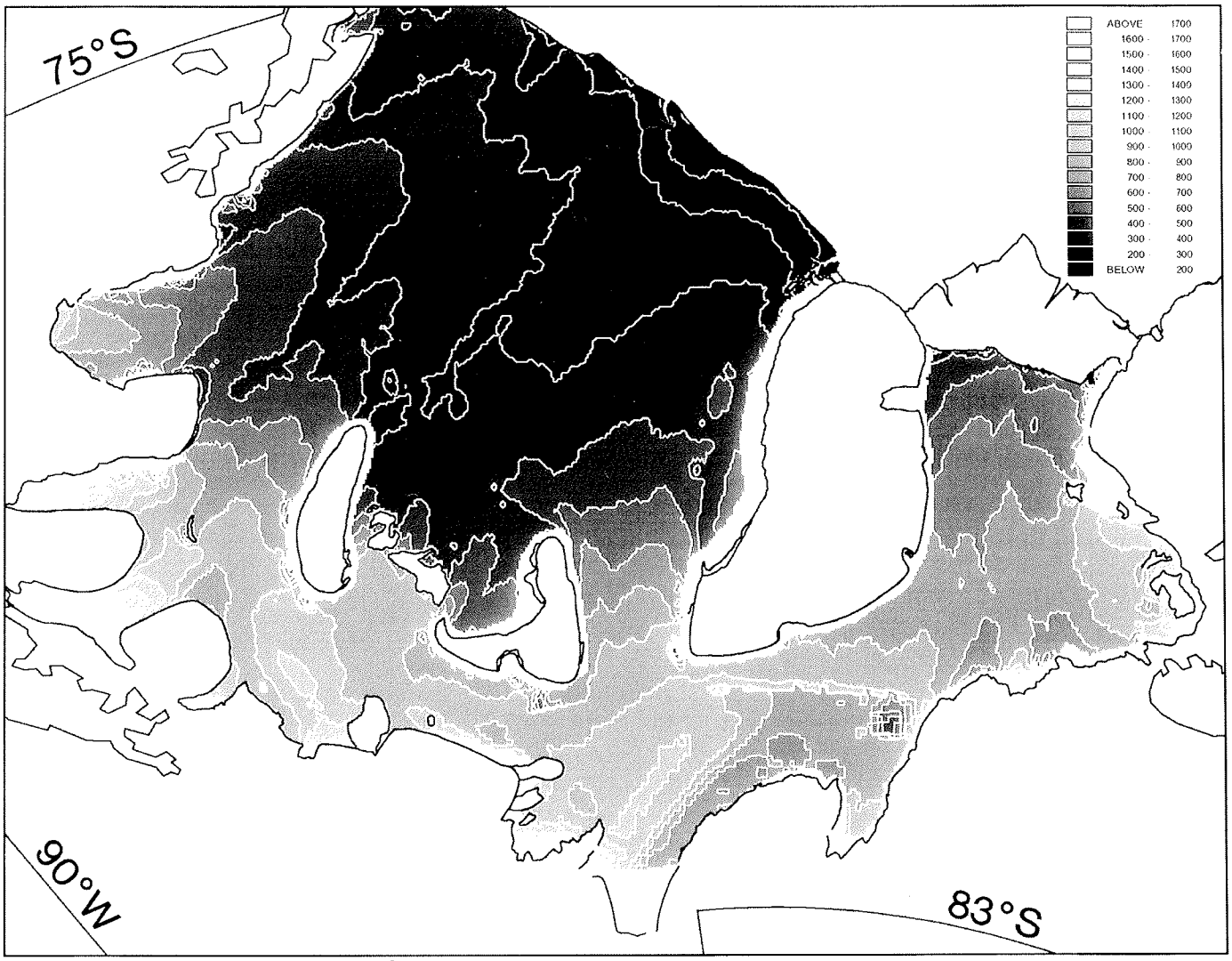

Fig. 3: Map of total ice thickness over Filchner-Ronne-Schelfeis. The discontinuity in ice shelf thickness at latitude 81.3° S marks the junction between ERS-1 and conventional elevation data.

Abb. 3: Karte der Gesamteismächtigkeit des Filchner-Ronne-Schelfeises. Die Diskontinuität in der Schelfeisdicke bei der geographischen Breite von 81.3° S markiert die Grenze zwischen den konventionellen und den ERS-1-Höhendaten.

are, however, problems specific to seismic techniques. The identification of the echoes and interpretation of the seismic returns is not always reliable in areas of active freezing where the base of the ice shelf may be indistinct due to a layer of unconsolidated ice slush (ENGELHARDT & DETERMANN 1987, NICHOLLS et al. 1991). The seismic coverage is also limited by logistic requirements and to areas accessible for ground based work; crevassed areas are generally beyond the scope of seismic work.

Thus over floating ice neither radar nor seismic sounding can be relied upon to produce a map of total ice thickness that is adequate for our requirements. We have chosen to invert surface altimetry from the ERS-1 satellite to produce a model of the total ice thickness. This approach has the advantage that most of the ice shelf, except for the portion south of 81.3° S (which is beyond the satellite's orbit), is covered with a high density of points in a consistent dataset from a single source. We assume that the ice shelf is in hydrostatic equilibrium, i.e. that the surface elevation, total thickness and draft are linearly related by functions of ice and sea water densities which were assumed to be constant, thickness becoming a linear function of surface elevation.

Processing of ERS-1 data

The surface elevation map derived from ERS-1 altimetry has already been presented by SIEVERS et al. (1995). Data from the fast delivery (1 Hz) data product (ERS-1.ALT.FDC) were processed at Mullard Space Science Laboratory, UK to retrieve the best ellipsoidal heights using only one cycle (Cycle 93) of the 35-day repeat orbit. During this period the instrument was operating in a high precision „ocean" mode. Waveform data are not included in this product and so retracking was not possible. The processing included removal of suspect data points and application of the Preliminary Orbit. Reliable atmospheric and

tidal corrections were not available and so none were applied. A crossover analysis showed residuals of around 1 m. Reduction of the data to orthometric height was carried out at Institut für Angewandte Geodäsie, Germany using Geodetic Reference System 1980, (Moritz 1984) and geopotential model OSU91A (Rapp et al. 1991). A final bias correction was made to bring the data into line with the most reliable ground-based data (trigonometric levelling).

The resulting map of ice shelf surface elevation shows vertical accuracy, calculated by Sievers et al. (1995) as ± 5 m, and good planimetric detail. Features as small as a 10 km wide „wake" of thin ice downstream of Kershaw Ice Rumples are clearly visible. There is a consistently high density of points across the whole ice shelf and the satellite has collected data over the areas of crevassing. The small area of floating ice shelf beyond the southerly limit of ERS-1 coverage (81.3° S) was filled in using data from the earlier elevation compilation also described by Sievers et al. (1995).

Hydrostatic conversion

Regionally, ice cannot support large shear stresses over long periods, thus floating ice shelves must be in regional hydrostatic equilibrium and we can derive ice thickness from ice surface elevation. For FRS, Jenkins & Doake (1991) showed a regression of elevations measured by Doppler satellite positioning on Ronne Ice Shelf against thickness and found a relationship of

$$h = 0.107H + 13 \quad (1)$$

gave a good fit to the data, where h is the surface elevation (WGS84) in metres, and H is the total ice thickness in metres. The intercept value of 13 m represents both a correction for the lower fim density, and an offset between the geoid model and true sea level.

To establish a conversion from ERS-1 surface elevation to total ice thickness we have derived a similar relation between a map of meteoric ice thickness originally presented by Crabtree & Doake (1986) but subsequently improved, and the surface elevation model derived from the ERS-1 data (Sievers et al. 1995). The two datasets were interpolated on to an identical 2 km grid and a comparison was made between corresponding gridpoints in 15 areas (Fig. 4a). The relation between thickness and surface elevation will only be linear in areas where we expect there to be only meteoric ice and no marine ice layer, outside areas of crevassing and areas of grounding. Several such areas (A-J) were selected, together with several areas (K-O) suspected of having a marine ice layer. Fig. 4b shows the variation of ERS-1 derived surface elevation with radar sounding ice thickness. We find that the data are well fitted by the straight line,

$$h = 0.108H + 17 \quad (2)$$

except in zones K-O which lie above the line, confirming the presence of a marine ice layer. The gradient of this line is consistent with a mean density of the water beneath the ice shelf of 1028 kg m^{-3} and a density of solid ice of 917 kg m^{-3}. The change in the intercept value from the value given by Jenkins & Doake (1991) is small and is possibly due to a systematic biases between the ERS-1 data and the thickness data.

The scatter about the line in Fig. 4b indicates that the relation given by Equation 2 is reliable to around 7 m in elevation and 70 m in thickness. The scatter is due to the combination of various uncertainties and errors:

a) Error in the ERS-1 altimetry, estimated by Sievers et al. (1995) as ± 5 m.
b) Error in the radar sounding data, due to the combined effects of our uncertainty in the speed of radio waves in ice, uncertainty of the correct firn correction and limitations of the digitising techniques. Additionally, there is a significant uncertainty in the navigation of track data. Crabtree & Doake (1986) found the standard mismatch at the cross-over points was ± 40 m of ice thickness.
c) Error due to gridding of radar data. This is extremely hard to quantify but is dependent on the distance from the nearest measurement point and spatial frequency of ice thickness variations.
d) Unknown accuracy of the OSU91A geoid in this area.
e) Systematic variations in the density of the ice shelf. Most of the ice column is close to maximum density but a small error may be introduced by changes in the firn structure across the region, especially were crevassing causes a reduced mean density for the upper layers (Sandhäger 1993). We estimate this at around ± 5 m in surface elevation.
f) Artifacts in the ERS-1 data (particularly off-pointing and snagging; Martin et al. 1983) cause the surface elevation given in the fast delivery product to be unreliable close to the ice shelf margins or where surface gradients are higher than on the ice shelf.

Combining the known error estimates from items (a), (b) and (e) gives a root mean square value of 8 m for the elevation error, but the dominant source of the error will vary from region to region. Thus in terms of precision of ice thickness this method does not represent an improvement over airborne radar sounding or seismic sounding; the value of the approach is improved coverage and spatial resolution.

Validation of the total ice thickness map

Figure 3 represents the hydrostatic conversion (Equation 2) applied to the surface elevation data presented by Sievers et al. (1995). Areas within 10 km of ice shelf grounding zones are not included. There are three boreholes on FRS that provide us with useful data for checking the map; the D335 hole described by Engelhardt & Determann (1987) and two holes described by Nicholls et al. (1991) and designated 90/1 and 90/2. Table 1 shows the comparison of the borehole data and thicknesses extracted from the map at these locations. The comparison of these measurements with the map of total ice thickness is satisfactory, all the errors being well within the limits claimed.

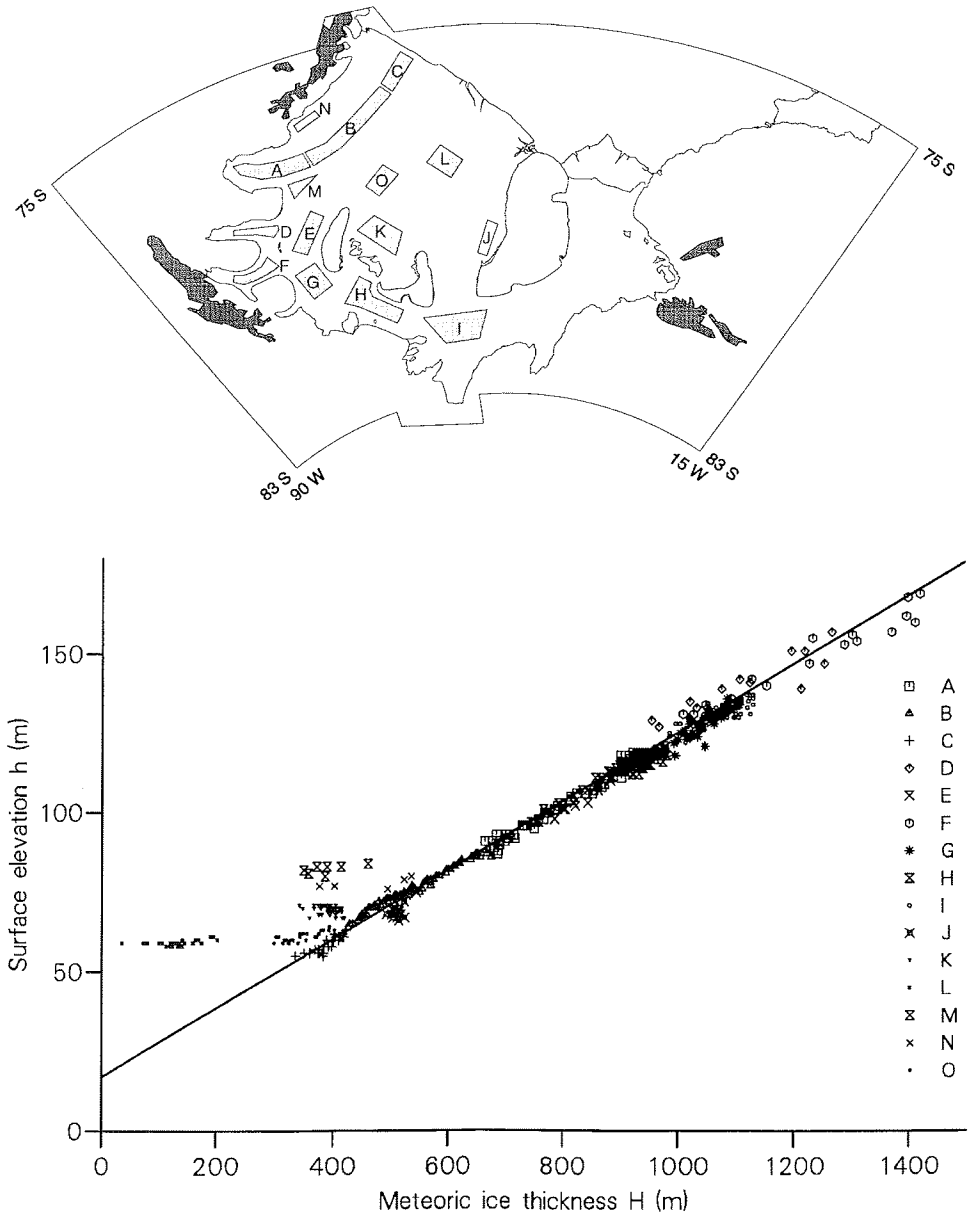

Fig. 4: Regression of ERS-1 surface elevations (OSU91A) and meteoric ice thickness. Top = areas of ice shelf from which data was taken. Bottom = relation between ERS-1 surface elevations h, and meteoric ice thickness H. The straight lines correspond to Equation (2). Zones A-J are believed to have no marine ice layer and yield points that lie close to the straight line. Zones K-O, are known or suspected of having some marine ice layer, and these yield points that lie above the straight line.

Abb. 4: Beziehung zwischen ERS-1-Oberflächenhöhe (OSU91A-Modell) und meteorischer Eisdicke. Oben = Schelfeisbereiche, die zur Berechnung herangezogen wurden. Unten = Beziehung zwischen ERS-1-Oberflächenhöhe h und meteorischer Eisdicke H. Die gerade Linie entspricht Gleichung (2). Die Zonen A-J besitzen vermutlich keine marine Eisschicht. Im Diagramm sind sie durch Punkte repräsentiert, die nahe an der Funktionsgeraden liegen. Bei den Zonen K-O ist bekannt oder wird vermutet, daß eine marine Eisschicht vorhanden ist. Punkte, die zu diesen Zonen gehören, liegen oberhalb dieser Geraden.

In addition the present ice thickness map was compared to two previous (and independent) maps of total ice thickness. These were prepared from seismic data (Pozdeev & Kurinin 1987) and airborne altimetry (Thyssen et al. 1993, Sandhäger 1993). The standard differences between the ERS-1 derived map and previous maps were 32 m and 34 m, respectively. These values are entirely consistent with the estimated uncertainty of the three maps.

4 DISCUSSION OF MAPS

Subglacial and seabed topographic map

General morphology

Pozdeev & Kurinin (1987) identified two major morphological provinces for the area they termed the *Weddell Sea shelf* and *the surrounding mountain frame*. This distinction is largely artificial, since we now suspect that the area comprises several distinct tectonic blocks (Johnson & Smith 1992). But we note that the seabed beneath the open sea is generally subdued (reflecting the thick sedimentary cover), while beneath the grounded ice there is a mountainous terrain, showing several uplifted blocks, and deep trenches filled by glaciers.

The subglacial and seabed elevation map (Appendix - main map) shows that the seabed topography is dominated by a gen-

tle downward slope towards the continent. Typically, the seabed is 1000 m lower at the grounding zone than beyond the ice front in the Weddell Sea. In several areas the bed is deepest along glacier troughs a few tens of kilometres inland of the grounding zone. This inland slope and trough near the grounding line is a common feature of Antarctic margins (TEN BRINK 1994). However, only a small portion of the inland slope can be ascribed to isostatic depression of the lithosphere by ice sheet loading. DREWRY & JORDAN (1983) estimated that the isostatic depression should vary from 50 m in the north to 200 m along the southern grounding zone. Other mechanisms that could lead to this pattern were listed by TEN BRINK & COOPER (1990). These were, the pattern of erosion, the pattern of sedimentation, sea level changes, thermal and tectonic subsidence and compaction of the sedimentary section by the ice cap. It has been suggested (TEN BRINK & SCHNEIDER 1994) that this trough is largely the combined effect of inner shelf erosion and outer shelf deposition.

The western margin of the Ronne Ice Shelf is characterised by extreme topography. DOAKE et al. (1983) noted that from the summit of Vinson Massif (5140 m ASL) to the trough beneath Rutford Ice Stream (1500 m below sea level) is a horizontal distance of only 45 km, resulting in a sustained gradient of 10 degrees. DOAKE et al. (1983) suggested that the three western ice streams (Evans, Carlson and Rutford) are located in grabens originally formed by NE/SW extension between the Ellsworth Mountains and the Antarctic Peninsula, and that these grabens were further emphasized by glacial erosion.

This view was clearly supported by aeromagnetic anomalies presented by GARRET et al. (1988) and modelling of deep crustal features that caused these anomalies by MASLANYJ & STOREY (1990).

Comparison of the subglacial topography of the hinterland of FRS (Appendix - main map) with that of the Siple Coast of Ross Ice Shelf (DREWRY & JORDAN 1983) shows marked differences. For the most part the ice streams entering FRS lie in deep bedrock troughs and are bounded by bedrock/geological features, whereas those on Siple Coast lie on a bed that shows little topography and little landward dip. In these respects the FRS „ice streams" more closely resemble East Antarctic glaciers, such as Jutulstraumen, Shirase Glacier, Lambert Glacier, Denman Glacier and Totten Glacier, which also lie in bedrock troughs and have beds that reach a maximum depth upstream of the grounding zone.

Another strong feature of the seabed is the Filchner Depression (also known as the Thiel Trough and Crary Trough). This is identifiable as a single feature from the continental shelf edge, under the Filchner-Schelfeis and along the eastern margin of Berkner Island, to the point at which the bedrock data runs out (around 80° S). Further south the picture is unclear. Filchner Depression is up to 1400 m deep, leading to a general acceptance that it is tectonic in origin. POZDEEV & KURININ (1987) suggested that the Filchner Depression continues south to become the „Southern Trough" passing to the south of Korff and Henry ice rises, and eventually joining to make a single continuous feature with the Ronne Depression. This might suggest that there is a distinct tectonic block beneath Berkner Island and Ronne Ice Shelf. There is, however, no bedrock data to support or deny this hypothesis. The present compilation shows a slightly shallower bed than that given by POZDEEV & KURININ (1987), but one that is at least 200 m deeper than the interpretation by DREWRY & JORDAN (1983). This does not imply that we believe Filchner Depression, Southern Trough and Ronne Depression to be in any way continuous or connected in origin. An alternative hypothesis is that Filchner Depression might actually be continuous and structurally allied to the trough beneath Foundation Ice Stream, or even to the smaller one beneath Support Force Glacier.

Beneath the west side of FRS lies the Ronne Depression, which is distinct but not so deep as Filchner Depression. It is bounded on the south-east by the submarine ridge, first noted by POZDEEV & KURININ (1987) and shown by NICHOLLS & JENKINS (1993) to be highly influential in the oceanographic evolution of the area. The submarine ridge extends inland from the ice front but may stop short of joining with the Fowler Peninsula. Under the current ice flow regime the submarine ridge is immediately downstream of Fowler Peninsula. It is seductive to envisage the submarine ridge as a relict of a grounded phase, during which ice streams eroded the bed to the east and west, but left a high in the wake of Fowler Peninsula. There is no particular magnetic anomaly in the region that might suggest that the ridge is an igneous body (MASLANYJ et al. 1991).

The floating portion of FRS is interrupted by several areas of grounded ice that rest on areas of high bedrock. Besides Berkner Island (which will be discussed in a separate section), there are four smaller ice rises and many ice rumples (Appendix - main map). Three of these, Korff Ice Rise, Doake Ice Rumples and Henry Ice Rise, occupy an influential central position in the ice shelf. All three grounded areas rest on a continuous bedrock shoal (later referred to as the KDH block).

A smaller point of grounding is Kershaw Ice Rumples. Here the ice shelf is around 1000 m thick when it impinges on bedrock that rises to a depth of around 500 m below sea level (SMITH 1986). It is notable that this point of rock effectively ploughs a furrow 20 km wide and 500 m deep into the base of the ice shelf at a rate of around 200 m a^{-1} (JENKINS & DOAKE 1991). Consequently it must suffer considerable erosional stress. If the bedrock feature causing this erosion were sedimentary, like the surrounding sea bed (JOHNSON & SMITH 1992) it would, in geological terms, be short-lived. Alternatively, the bedrock feature might be a more robust igneous body protruding though the sedimentary cover. This interpretation is supported by the aeromagnetic anomaly map by JOHNSON et al. (1992), which shows an isolated dipole anomaly of several hundred nT centred on Kershaw Ice Rumples. If this interpretation is correct then the rise forming Kershaw Ice Rumples may be significant when modelling ice flow in this area. There is at present little data to indicate the depth of the bed beneath Hemmen Ice Rise, or its likely origin.

Evidence for structure of former ice sheets

The seismic stratigraphy of the continental shelf in the Weddell Sea shows strong evidence of several phases during which the grounded ice sheet extended to the continental shelf break (KUVAAS & KRISTOFFERSEN 1991). Using lithologies from 83 cores, ELVERHØI (1981) found that stiff pebbly mud (interpreted as till deposits from a grounded ice sheet) was overlaid by a veneer of soft pebbly mud (interpreted as glaciomarine deposits). He went on to suggest a late Wisconsin age for the advance of the grounded ice sheet to a depth of 500 m at the continental shelf break around 30,000 ka bp. This interpretation was, however, based on only one ^{14}C date from a shell fragment, and so must be treated with caution. Although, assuming only that the West Antarctic Ice Sheet has been grounded out to the continental shelf break during some period, it is reasonable to expect some evidence of a grounded glaciation to remain beneath FRS. It is notable that the ice sheet would have been grounded on the bedrock plain that is now seaward of the ice front and covered with sedimentary material. Although we have argued above that the present configuration of the ice streams entering FRS is very unlike the Siple Coast of Ross Ice Shelf, we can see that the structural style of this earlier configuration might have borne considerably more resemblance to the present day Siple Coast.

Fig. 5 shows a shaded relief of the bedrock around the FRS. The image is calculated from the gridded bedrock data as if the bed were a Lambertian scatterer illuminated from a direction 35° anticlockwise from the y-axis (approximately north-west). The major features are clearly visible, the smooth „plain" beneath Ronne Ice Shelf, the mountainous frame, and the uplifted blocks on which Berkner Island and the Korff/Doake/Henry system rest. Unfortunately, several artifacts in the gridded values are also present. Close to the ice front where the bedrock compilation included very dense point data that had considerable uncertainty, the shaded relief image shows a pocked texture. Several very noticeable pockmarks are due to specific seismic measurements and may be an artifact of observation noise. Conversely, where data are very sparse (for example in Zone H) the image has a faceted appearance, betraying the triangulation method used to produce the grid. Finally, where the compilation included contour data, the image is particularly smooth, reflecting the smoothing during production of the contour data.

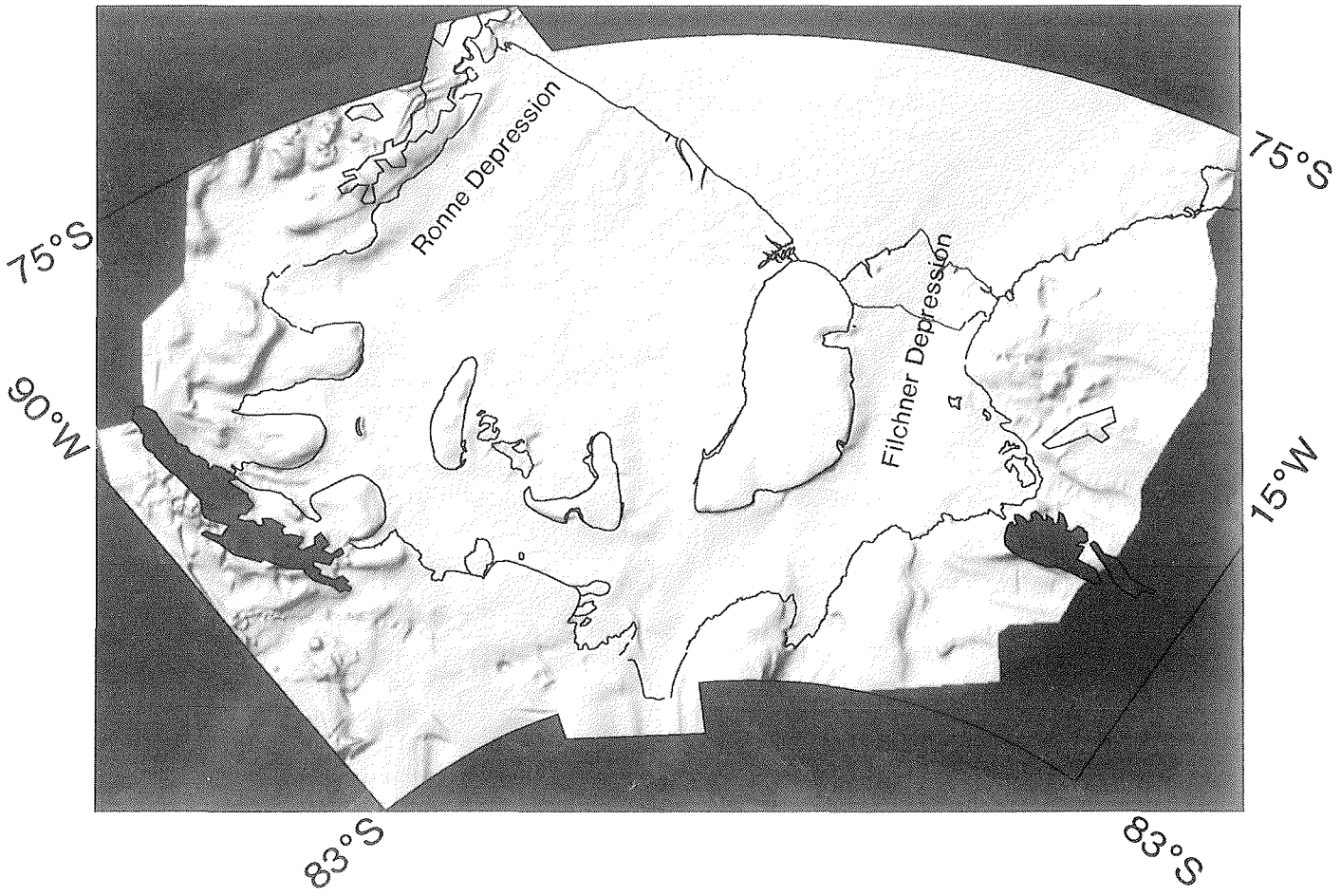

Fig. 5: Shaded relief of the bedrock in the Filchner-Ronne-Schelfeis region. Constructed using a Lambertian scattering model and an illumination direction of 315°, (from the top-left).

Abb. 5: Schummerung des Meeresboden- und Eisuntergrundreliefs im Gebiet des Filchner-Ronne-Schelfeises. Hergestellt mittels eines Lambertschen Beleuchtungs- und Streumodells und einer Beleuchtungsrichtung von 315° (aus Nordosten).

The angle of illumination on Fig. 5 was chosen to accentuate structures parallel to the flow direction beneath FRS and so highlight relict glacial structures beneath the ice shelf, either erosional or depositional. The trough between Berkner Island and Henry Ice Rise might be glacial in origin, carved by the Möllereistrom/Foundation Ice Stream unit during a grounded phase. Similarly the Ronne Depression closely follows the present flow of Evans Ice Stream and may be a relict of erosion by this glacier. To the east of Berkner Island and north of Korff and Henry ice rises the sea bed is particularly smooth. This is consistent with the interpretation of magnetic anomalies by JOHNSON & SMITH (1992) that in this area the ice shelf is underlain by up to 15 km of sedimentary and metasedimentary rock, thinning to 2 km near Berkner Island. We should expect that during earlier periods of grounding these sedimentary sequences would have suffered erosion and still bear the scars of such events. Seismic reflection sections from the west Ronne Ice Shelf show an unconformity close to the surface confirming erosional episodes (E. KING, pers. comm. 1991).

It is not possible to resolve the history of ice sheet advance and retreat from the sea-bed topography alone, we must await detailed modelling and geophysical investigations. Several important points can, however, be concluded with only a simple-minded interpretation. The importance of the KDH block in the evolution of FRS is emphasised by the disparity of results from models which either restrict or allow free flow across Doake Ice Rumples. Even a small drop in sea-level might cause a merging of these grounding features, completely diverting flow around the KDH block. This implies, for example, that the palaeo-flowlines for a grounded-phase ice sheet, shown by STUIVER et al. (1981: 419) are particularly unlikely since the KDH block would have barred the route suggested. A more likely scenario is the splitting of flow into three ice streams or ice shelves; one in the Ronne Depression, another between the KDH block and Berkner Island and the last in the Filchner Depression. Beyond the ice front two of these troughs extend a considerable distance towards the continental shelf break, probably indicating the routes for the major glaciers during a grounded-phase. The third bedrock trough, between Berkner Island and Henry Ice Rise, appears to be less well developed and ends somewhere in the centre Ronne Ice Shelf. It is possible that there is a connection (not clearly shown on Appendix - main map) to Ronne Depression across the submarine ridge, or that this glacier was only active during an intermediate phase of ice sheet extent.

The morphology of Berkner Island

Berkner Island has two domes; in the north, Reinwarthhöhe more than 650 m above sea level, and in the south, Thyssenhöhe more than 850 m above sea level (THYSSEN & HOPPE 1988, SANDHÄGER 1993). Although the ridge between the summits does not drop below 550 m a.s.l., the two domes are distinct and may have different glaciological histories.

The subglacial topography (Appendix - main map) and the earlier work by THYSSEN & HOPPE (1988) and SANDHÄGER (1993) shows that bedrock topography beneath Berkner Island is highly asymmetric. The highest point of the bedrock, almost directly beneath the southern dome (Thyssenhöhe), is less than 50 m below sea level. Beneath both the domes there is a gentle westward gradient on to the plain beneath the northern Ronne Ice Shelf, and on the eastern margin of Berkner Island there is a steeper eastward gradient into the Filchner Depression, which reaches around 3° in the north, and around 10° in the south (see Appendix - main map). As a result of these steep gradients, the horizontal position of the eastern margin of Berkner Island will be relatively stable to significant changes in sea level, of say 100 m. The western margin of Berkner Island is rather different. Under the northern dome (Reinwarthhöhe) the bedrock shelves gently westwards and the ice rise margin is not fixed by a steep bedrock gradient. Further south the westward gradient steepens, roughly coincident with the ice rise margin, but the bedrock gradients are never comparable with those on the eastern side.

The importance of this difference between the eastern and western margins of Berkner Island is highlighted if we consider that a 100 m fall in sea-level, or similar ice shelf thickening, would cause a rapid westward migration of the margin of perhaps 350 km, as the ice shelf grounds on bedrock shoals. We are not suggesting such events for any particular period, simply using the point to illustrate that the western margin of Berkner Island is unusually prone to migration.

REEH (1982), showed that assuming a plastic rheology and without a strong trend in bedrock an ice divide should occur equidistant from the margins. MARTIN (1976) performed an experiment where sand was poured onto a platform with a complex shape reminiscent of an idealized ice rise. With the further addition of sand, a maximum load was reached when the maximum supportable slope was reached over almost the whole area. Positions of the divides in this maximal system were easily observed under low angle illumination. REEH (1982) went on to show that for the central Greenland Ice Sheet where there is a strong bedrock trend, the position of the ice divide is drawn towards the bedrock ridge. This is a result of the driving stress being dependent on both surface and bed slope and can be seen also on the south dome (Thyssenhöhe) of Berkner Island.

The analogue experiment shown by Martin can be achieved digitally. Given the shape of the margin of an ice cap, it is an easy procedure to draw „contours of continentality", i.e. lines joining points equal distance from the margins. Fig. 6a shows measured ice surface elevation contours, reproduced from SIEVERS et al. (1993), together with the network of divides interpreted from the contours and Landsat imagery. Fig. 6b shows contours of continentality for Berkner Island. For this exercise the margin is taken to be the grounding line shown by SWITHINBANK et al. (1988). These contours were drawn using the „buffering" algorithm available in the Laserscan Horizon GIS package. Contours of continentality correspond to the elevation contours predicted by Reeh's plastic ice sheet model, assuming a flat ice sheet bed. The network of divides corresponding to these contours is also interpreted by hand. A comparison of the positions of ice divides

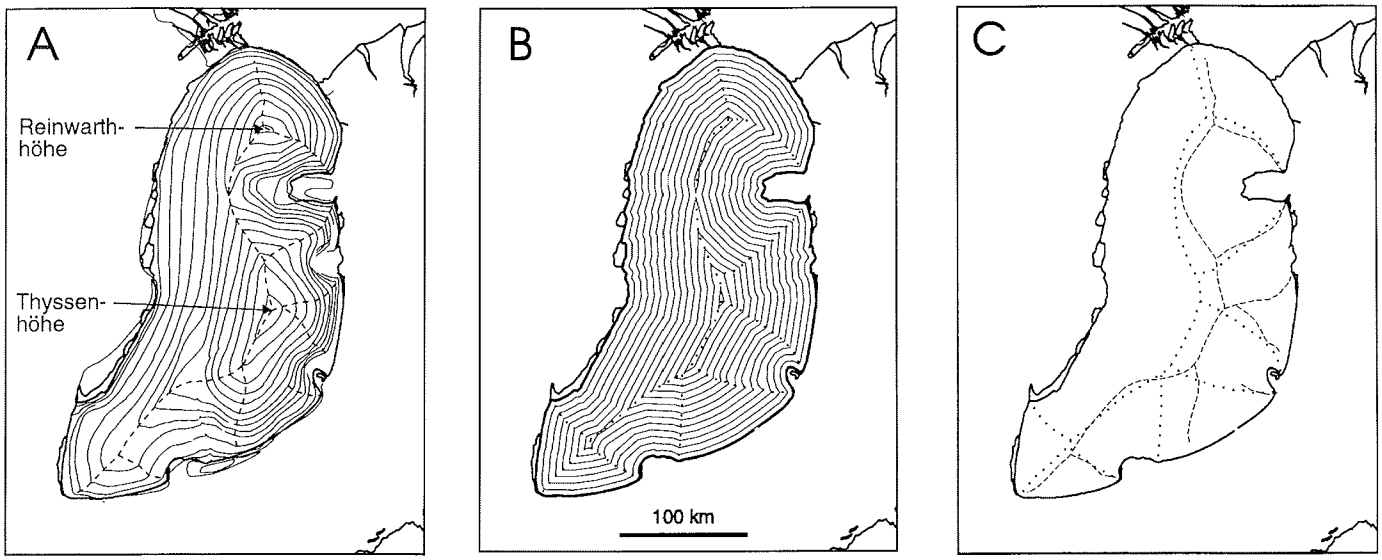

Fig. 6: Comparison of observed ice sheet topography and ideal flat bed/plastic ice sheet topography over Berkner Island. A = surface elevation contours taken from SIEVERS et al. (1993). Ice divides indicated by dashed lines were drawn by hand. B = contours of continentality calculated using the margin of grounded ice given in SWITHINBANK et al. (1988). C = comparison of observed ice divides (dashed lines) and predicted ice divides (dotted lines). Note the maximum disagreement between the observed and predicted divide positions occurs in the region of the southern dome (Thyssenhöhe).

Abb. 6: Vergleich der Topographie der real vermessenen Eisoberfläche von Berkner Island mit der modellierten Oberfläche eines plastischen Eiskörpers auf ideal flachem Untergrund. A = Höhenlinien der realen Eisoberfläche aus SIEVERS et al. (1993), mit eingezeichneten Eisscheiden. B = Linien gleichen Abstands von der Aufsetzlinie („contours of continentality"), berechnet mit Hilfe der Aufsetzlinie aus SWITHINBANK et al. (1988). C = Vergleich von beobachteten Eisscheiden (gestrichelte Linien) mit modellierten Eisscheiden (gepunktete Linien). Die größten Abweichungen treten im Gebiet der Thyssenhöhe auf.

and summits from the plastic model (contours of continentality) and real data will show the distortion of the ice cap due to bedrock topography and perhaps other effects (e.g. basal sliding or patterns of accumulation). Fig. 6c shows the network of ice divides and ridges that are implied by the continentality procedure from Figs. 6a and b. We can see that the networks are in fact topologically similar, but there is a general shift and distortion. The southern dome (Thyssenhöhe) is displaced at least 20 km, while the north dome (Reinwarthhöhe) is only around 8 km from the predicted centre. The pattern of distortion is a reflection of the severe topography beneath Thyssenhöhe, compared to the gentler topography beneath Reinwarthhöhe.

Water column thickness map

The picture shown by the water column thickness map (Appendix - inset map) is of a highly complex water cavity. The water column is at it thickest in the Filchner Depression (>700 m) and in the Ronne Depression (>500 m). These are very deep bodies of water; globally the average depth at the continental shelf break is around 130 m (PICKARD 1979: 9). Conversely, the water column thickness map shows a 100 km swath west of Berkner Island, and inland from the ice front where the water column is generally less than 200 m. Within this swath there are at least four areas where the clearance between the ice shelf base and the seabed is less than 100 m. With the present interpretation of the bedrock south of the KDH block, the path of maximum water column thickness from Ronne Depression to the Filchner Depression passes north of the KDH block.

The map of the water column thickness may help oceanographic, tidal and glaciological modellers. HELMER & OLBERS (1991) noted that their model of oceanographic flow beneath FRS was particularly sensitive to the model domain, and it is now clear that their idealised domain was far from representative. NØST & FOLDVIK (1994) assumed that a deep channel ran from Ronne Depression round the southern side of the KDH block and joined with the Filchner Depression. Although the map indicates that such a channel may exist, we emphasise that very little data have been collected to support this conclusion.

The observation that the clearance between the ice shelf base and the seabed close to the ice front of Ronne Ice Shelf narrows to less than 100 m in four areas, raises the question: can the ice shelf ground here while remaining afloat further inland? If we assume that local grounding would have a damming effect and lead to further thickening and more grounding, this would lead to grounding across about two-thirds of the Ronne ice front. Beneath most of Filchnerschelfeis (except the seabed plain around the mouth of Bailey Ice Stream) the water column thickness is much greater and so this ice shelf is much less prone to grounding.

Oceanography

Three oceanographic transects across the ice front of FRS have been published and although they were all collected in the summer months they span more than a decade, 1980 (FOLDVIK et al. 1985), 1984 (ROHARDT 1984) and 1993 (GAMMELSRØD et al. 1994). GAMMELSRØD et al. (1994) discussed the differences be-

tween these transects, we attempt to summarise the similarities and what we might conclude from them.

Both ROHARDT (1984) and FOLDVIK et al. (1985) identified three cores of water at less than -2 °C across the Ronne ice front (Fig. 7a). These cores are in a similar position in both sections, one in Ronne Depression 58.5° W, which we designate (A); a second, coincident with the submarine ridge at 56.5° W, designated (B) and the third at roughly 54.5° W designated (C). GAMMELSRØD et al. (1994) observed the same cold cores but (perhaps due to an unfortunate distribution of stations around the submarine ridge) failed to differentiate between cores A and B. Furthermore, all the sections showed that the tops of the cold cores were consistently at 100-200 m depth, coincident with the ice shelf base.

FOLDVIK et al. (1985) showed the thickness of the cores were around 200 m and identified these cores as Ice Shelf Water (ISW) emerging from beneath the ice shelf. Since the plumes emerge at the level of the ice shelf base, two (B and C) appear to fill the whole water column at this point. There is little evidence presented here, for the detachment of the ascending plume from the ice shelf base (JENKINS & DOAKE 1991).

Similarly, all the sections showed a core of warm water (between -1.45 °C and - 1.6 °C) at around 53° W. GAMMELSRØD et al. (1994) noted that the warm core appeared to be a „permanent" feature, but the exact location and size of this core was far more variable than for the cold cores. Both FOLDVIK et al. (1985) and GAMMELSRØD et al. (1994) identified this core as Modified Weddell Deep Water (MWDW) entering the subice shelf cavity.

These observations have been widely interpreted in terms of a thermohaline circulation beneath the ice shelf which produces cold Ice Shelf Water (eg. NØST & FOLDVIK 1994). The observation that the cores appear to be fixed over many years implies that the positions of the cores are controlled by features of the seabed and/or ice shelf, and that there are favoured routes of escape for ISW from the sub-ice cavity. Similarly, the approaching MWDW is constrained by the Weddell Sea bathymetry. The maps presented here allow us to look for these topographic controls by considering correlations with the three parameters, ice shelf draft, water column thickness and seabed topography.

A major feature of the bathymetry north of Ronne Ice Shelf front is a westwards dipping scarp (-350 to -450 m) unbroken from the ice front to the shelf-break. A southwards flowing bottom current of MWDW produced near the shelf-break (deflected left by the Coriolis Force) might rest against this scarp, and so enter the ice shelf cavity just west of 52-53° W. This is indeed the position indicated on the sections for the MWDW core (Fig. 7a)

ISW emerging from beneath an ice shelf may be buoyant and so whilst beneath the ice shelf we might expect it to be directed by features of the ice shelf base or perhaps the water column thickness. To investigate these relations, the positions of cores A, B and C (FOLDVIK et al. 1985) have been overlaid with con-

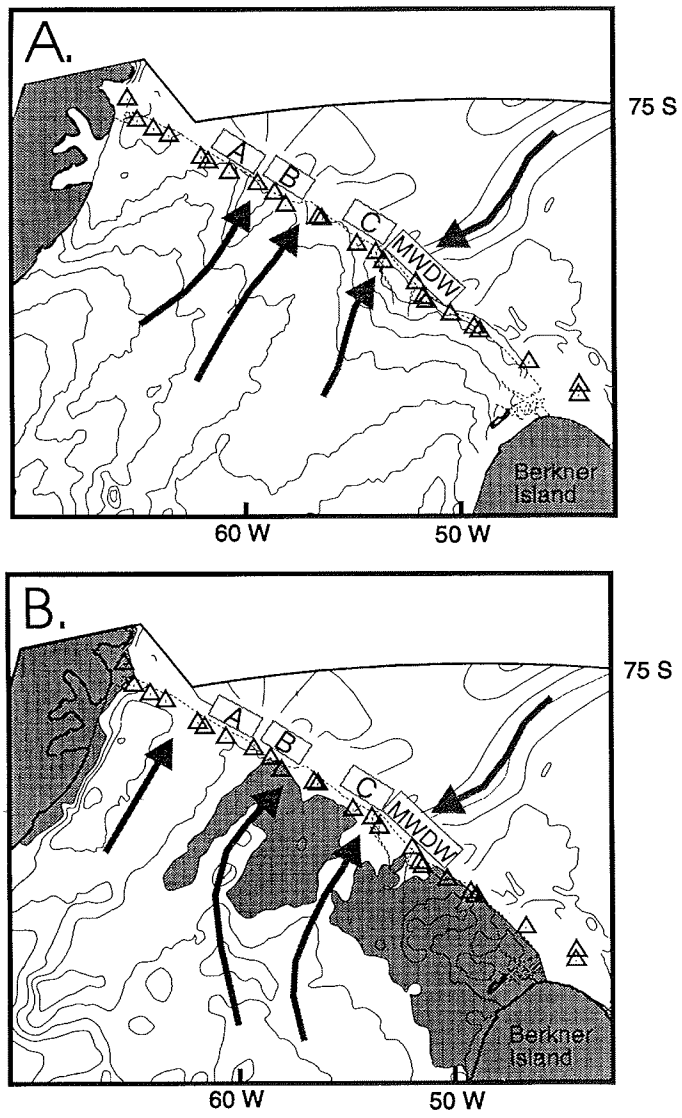

Fig. 7: Oceanographic sketches of Ronne Ice Shelf showing the position of conductivity, temperature and depth observations by FOLDVIK et al. (1985) marked by triangles, and the cores of water identified. A, B and C are cores of Ice Shelf Water emerging from the ice front and MWDW is the core of Modified Weddell Deep Water approaching the ice front. Beyond the ice shelf front, are contours of sea bed depth and the proposed path of the MWDW following the westward dipping scarp to the continental shelf-break. A: shows contours of total ice thickness over the ice shelf. Three troughs in the ice shelf base that might be expected to direct buoyant plumes of ISW are indicated by the arrows. The positions at which these channels emerge from the ice front do not coincide well with the ISW core positions. B: shows contours of water column thickness, shaded where less than 200 m. The arrows indicate the three routes with the thickest water column connecting the interior cavity with the open sea.

Abb. 7: Lage der CTD-Profile (contactivity, temperature, depth) vor dem Ronne Ice Shelf (Dreiecke, aus FOLDVIK et al. 1985). A, B und C sind Kerne mit Schelfeiswasser, das unter der Eisfront austritt. MWDW ist der Kern des Modified Weddell Deep Water, das sich der Eisfront nähert. A = Isolinien der Gesamteismächtigkeit des Schelfeises. Drei kanalartige Aushöhlungen an der Schelfeisunterseite, die möglicherweise Schelfeiswasserfahnen lenken, sind durch Pfeile gekennzeichnet. Die Stellen, an denen diese Kanäle aus der Eisfront austreten, fallen nicht genau mit der Lage der beobachteten Schelfeiswasserkerne zusammen. B = Isolinien der Wassersäulendicke, die schraffiert ist, wenn sie weniger als 200 m beträgt. Die Pfeile zeigen die drei Verläufe mit der größten Wassersäule unter dem Schelfeis, die die innere Höhlung mit der offenen See verbinden. Vor der Schelfeisfront sind Höhenlinien des Meeresbodens dargestellt sowie der vermutete Verlauf des MWDW entlang des westlichen Steilabfalls vom kontinentalen Schelf.

tours of ice shelf thickness and water column thickness (Fig. 7). Figure 7a shows that there are four channels of thin ice, but that the cores A, B and C appear to emerge from beneath the keels between the troughs of thin ice, rather than from the troughs.

Comparison of the position of the cores with the water column thickness is similarly inconclusive. The water column thickness map shows two channels from the central area to the ice front, in which the water column is continuously greater than 200 m (Fig. 7b). One of these is over the Ronne Depression and the other emerges at 54° W. A third channel thins to less than 200 m around 30 km short of the ice front, but emerges at around 57° W. Core A sits in the Ronne Depression channel, core C emerges at the mouth of the channel at 54° W, and core B might be associated with the thinner channel at 57° W. We conclude that the positions of the cores of ISW may be controlled, at least in part, by the available channels of escape from beneath the ice shelf as indicated by the map of water column thickness. It would be too simplistic to expect that either ice shelf draft or water column thickness could entirely explain the positions of the ISW cores, and this will require analysis using a full three-dimensional thermohaline model.

Vertical Cross-sections

To emphasise some of the points made earlier and to aid visualisation we discuss representative ice shelf and water column profiles along five cross-sections, two roughly parallel to the ice front and three approximately following the ice flow from the main glaciers (Appendix - vertical cross-sections). The exact positions of the sections are shown in Appendix - sources diagram and inset map of sub-ice shelf water column thickness.

Section a-a' is roughly parallel to the front of the Ronne Ice Shelf and Filchnerschelfeis, around 20 km inland from the 1987 front position. The section shows Filchner Depression extending across the whole of the Filchnerschelfeis front, while the Ronne Depression extends only over the most westerly 150 km of Ronne Ice Shelf front. The eastern edge of the latter depression is marked by the submarine ridge. Between the submarine ridge and Berkner Island there is an apparently undulating seabed that leaves a water column generally less than 200 m thick and in places less than 100 m thick. Even a modest increase in the ice shelf thickness would cause grounding. The western margin of Berkner Island is not well defined and a westward migration of the ice rise would be likely with even a slight drop in sea level or increase in ice thickness.

Section b-a' is roughly perpendicular to the ice flow. It shows the Ronne and Filchner Depressions and the submarine ridge at it most prominent point (x = 200 km). b-b' is 250 km from the ice front, but the submarine ridge still rises to within 100 m of the base of the ice shelf and would require only a 20 % increase in ice thickness to cause grounding. Between the submarine ridge and Berkner Island there is a greater water column thickness of 400-600 m than across a-a' which is closer to the ice front. At this position the western margin of the bedrock block beneath Berkner Island is much steeper than in Section a-a'.

Section c-c' follows the approximate ice flowline studied by JENKINS & DOAKE (1991) from the grounding line of Rutford Ice Stream to the ice front and beyond into the open sea. The section shows that close to the grounding zone of Rutford Ice Stream the ice is around 1600 m thick, probably the thickest on FRS. Apart from the region close to the grounding line where SMITH & DOAKE (1994) have collected seismic data, the area up to 350 km lies in our data hole (Zone H of Appendix - sources diagram). The seabed bump at 340 km is the periphery of the feature causing Kershaw Ice Rumples.

Section d-d' follows the present ice flowline from the mouth of Foundation Ice Stream to the 1987 ice front and beyond into the open sea. The section shows that the ice shelf thins consistently along its profile, and that it is particularly close to grounding at the ice front. In both Sections c-c' and d-d', the ice front is within 30 km of the shallowest seabed.

Section e-e' follows the flowline from the grounding line of Recovery Glacier to the 1987 ice front and out into the open sea, and highlights the differences between Ronne Ice Shelf and Filchnerschelfeis. At the grounding line of Recovery Glacier the ice is a little less than 1000 m thick and there is little thinning along the flowline until within 80 km of the ice front. The thickness gradient on Ronne Ice Shelf is considerably higher. This ice shelf profile is probably a result of convergent flow over much of the ice shelf caused by the lateral constriction of the sides.

5 CONCLUSIONS

On the eastern side of Ronne Ice Shelf there is about 100 m of clearance between the base of the ice shelf and the sea bed. The profile along the contemporary flowline of Foundation Ice Stream shows that the ice shelf would ground with only a small increase in its thickness. Increased back-stress from the near ice front grounding point would increase ice thickness and grounding upstream. This would effectively block the current route of entry for MWDW and the exit routes associated with ISW cores B and C, with a possible consequence for the production of AABW.

The relative position of Berkner Island and the ice front is perhaps significant, since ice fronts often appear to be adjacent to pinning points. Across the eastern two thirds of Ronne Ice Shelf front there is an approximate juxtaposition (to within about 50 km) between the ice front and the highest area of the seabed topography. Although this juxtaposition may be coincidental, the geometry of the coastline means that the present day position of the ice front is metastable in the sense that any movement, either advance or retreat, results in a greater length. SANDERSON (1979) showed that an equilibrium ice shelf could only exist in a diverging bay without pinning points if the di-

Borehole			Total	ERS-1 Elevation (m)	ERS-1 Ice (m)	Map error (m)
D335	(78.309°S	57.128° W)	430*	61	407	-23
90/1	(77.597° S	65.467° W)	548	73	518	-30
90/2	(76.705° S	64.921° W)	541	77	555	14

Tab. 1: Comparison of ERS-I derived total ice thickness map with borehole data. * Although, the total ice thickness measured was 465 m, the last 35 m were interpreted as slush layers.

Tab. 1: Vergleich der Gesamteismächtigkeiten, abgeleitet aus ERS-1-Altimeterdaten, mit Ergebnissen aus Schelfeisbohrungen. * Die gesamte gemessene Eismächtigkeit beträgt 465 m, von der jedoch 35 m als Eisschlammschicht an der Schelfeisunterseite interpretiert werden.

vergence angle was less than a critical value, which depended on the ice thickness and velocity. Any advance of the Ronne Ice Front might immediately exceed this notional critical angle and cause the ice shelf to separate from the sides and calve back to near its present position. Indeed, SWITHINBANK et al. (1988) does show that over the last 30 km toward the ice front, the ice shelf becomes detached from the grounded ice sheet. The position of the shallowest point on the seabed might therefore be controlled by erosion and sedimentation associated with the ice front.

6 ACKNOWLEDGMENTS

The project was undertaken under the auspices of the Filchner-Ronne Ice Shelf Programme (FRISP), which is a sub-committee of the Scientific Committee for Antarctic Research (SCAR) Working Group on Glaciology. We should like to thank numerous colleagues for helpful discussions and to all those who helped in the collection of data. The gridded dataset representing the bedrock elevation and water-column thickness are available on request from the first author.

References

Bombosch, A. & Jenkins, A. (1995): Modelling the formation and deposition of frazil ice beneath Filchner-Ronne Ice Shelf.- J. Geophys. Res. 100: 6893-6992.

Carmack, E.C (1990): Large-scale physical oceanography of polar oceans.- In: W.O. SMITH Jr. (ed.), Polar Oceanography, part A, Phys. Sci. Pub. Academic Press, San Diego, 171-222.

Crabtree, R.D. & Doake, C.S.M. (1986): Radio-echo investigations of Ronne Ice Shelf.- Ann. Glaciol. 8: 37-47.

Doake, C.S.M, Crabtree, R.D. & Dalziel, I.W.D. (1983): Subglacial morphology between Ellsworth Mountains and the Antarctica Peninsula: new data and tectonic significance.- In: R.L. OLIVER, P.R. JAMES and J.B. JAGO (eds.), Antarctic Earth Science, Pub. Austr. Acad. Science, Canberra, 270-273.

Doake, C.S.M. & Vaughan, D.G. (1991): Rapid disintegration of Wordie Ice Shelf in response to atmospheric warming.- Nature 350: 328-330.

Drewry, D.J. & Jordan, S.R. (1983): The bedrock surface of Antarctica. - Glaciological and Geophysical Folio Series, Sheet 3, Scott Polar Res. Inst., Cambridge.

Elverhøi, A. (1981): Evidence for a late Wisconsin glaciation of the Weddell Sea.- Nature 293: 641-642.

Engelhardt, H. & Determann, J. (1987): Borehole evidence for a thick layer of basal ice in the central Ronne Ice Shelf.- Nature 327: 318-319.

Fahrbach, E., Augstein, E. & Olbers, D. (1994): Impact of shelf and sea ice on water mass modifications and large-scale oceanic circulation in the Weddell Sea.- In: G. HEMPEL (ed.), Antarctic Science, Springer-Verlag, Berlin, 167-187.

Ferrigno, J.G. & Gould, W.G. (1987): Substantial changes in the coastline of Antarctica revealed by satellite imagery.- Polar Record 23: 577-583.

Foldvik, A. & T. Gammelsrød, 1988. Note on Southern Ocean hydrography, sea-ice and bottom water formation. - Palaeogeography, Palaeoclimate and Palaeoecology, 67, 3-17.

Foldvik, A., Gammelsrød, T. & Torresen, T. (1985): Circulation and water masses on the Southern Weddell Sea shelf.- In: S.S. JACOBS (ed.), Oceanology of the Antarctic Continental Shelf, Antarct. Res. Ser. v. 43: 5-20, AGU Washington, D.C.

Fox, A. & Cooper, A.P.R. (1994): Measured properties of the Antarctic ice sheet derived from the SCAR Antarctic digital database.- Polar Record 30: 201-206.

Gammelsrød, T, Anderson, L.F., Fogelkvist, E., Foldvik, A., Jones, E.P., Nøst, O.A., Olsson, K., Skagseth, Ø., Tanhua, T. & Østerhus, S. (1994): Distribution of water masses over the continental shelf in the Southern Weddell Sea.- Geophys. Monogr. 84: 159-176.

Garret, S.W., Maslanyj, M.P. & Damaske, D. (1988): Interpretation of aeromagnetic data from the Ellsworth Mountains - Thiel Mountains ridge, West Antarctica.- J. Geol. Soc. Lond. 145: 1009-1017.

Giovinetto, M.B. & Bentley, C.R. (1985): Surface balance in ice drainage systems of Antarctica.- Ant. Journ. US., 20: 6-13.

Helmer, H.H. & Olbers, D.J. (1991): On the thermohaline circulation beneath the Filchner-Ronne Ice Shelves.- Ant. Sci. 3: 433-442.

Hinze, H. (1994): Charting the bathymetry of Weddell Sea, Antarctica.- Marine Geodesy 17: 139-145.

Jenkins, A. (1991): A one-dimensional model of ice shelf-ocean interaction.- J. Geophy. Res. 96: 20671-20677.

Jenkins, A. & Doake, C.S.M. (1991): Ice-ocean interaction on Ronne Ice Shelf, Antarctica.- J. Geophy. Res. 96: 791-813.

Johnson, A.C., Aleshkova, N.D., Barker, P.F., Golynsky, A.V., Masolov, V.N. & Smith, A.S. (1992): A preliminary aeromagnetic anomaly compilation map for the Weddell province of Antarctica.- In: Y. YOSHIDA (ed.), Recent Progress in Antarctic Earth Science, Terra Sci. Publ. Co., Tokyo, 545-553.

Johnson, A.C. & Smith, A.S. (1992): A new aeromagnetic map of West Antarctica (Weddell Sea Sector): introduction to important features.- In: Y. YOSHIDA (ed.), Recent Progress in Antarctic Earth Science, Terra Sci. Publ. Co., Tokyo, 555-562.

Kuvaas, B. & Kristoffersen, Y. (1991): The Crary Fan: a trough-mouth fan on the Weddell Sea continental margin, Antarctica.- Mar. Geol. 97: 345-362.

Mantyla, A.W. & Reid, J.L. (1983): Abyssal characteristics of the World Ocean water.- Deep Sea Res. 95: 1641-1654.

Martin, T.V., Zwally, H.J., Brenner, A.C. & Bindschadler, R.A. (1983): Analysis and retracking of continental ice sheet radar altimetry waveforms.- J. Geophys. Res. 88: 1608-1616.

Martin, P.J. (1976): Ridges on Antarctic ice rises.- J. Glaciol., 17: 141-144.

Maslanyj, M.P. & Storey, B.C. (1990): Regional aeromagnetic anomalies in Ellsworth Land: crustal structure and Mesozoic microplate boundaries within west Antarctica.- Tectonics 9: 1515-1532.

Maslanyj, M.P., Garret, S:W., Johnson, A.C., Renner, R.G.B. & Smith, A.M. (1991): Aeromagnetic anomaly map of West Antarctica (Weddell Sea Sector).- BAS Geomap Series, Sheet 2. 1: 2 500 000. Publ. British Antarctic Survey, Cambridge.

Moritz, H. (1984): Geodetic Reference System 1980.- Bull. Geod. Paris. 58: 388-398.

Nicholls, K.W. & Jenkins, A. (1993): Temperature and salinity beneath Ronne Ice Shelf, Antarctica.- J. Geophys. Res., 98: 22553-22568.

Nicholls, K.W., Makinson, K. & Robinson, A.V. (1991): Ocean circulation beneath Ronne Ice Shelf.- Nature 354: 221-223..

Nøst, O.A. & Foldvik, A. (1994): A model of ice shelf-ocean interaction with application to the Filchner-Ronne and Ross Ice Shelves.- J. Geophys. Res. 99: 142431-4254.

Oerter, H., Eicken, H., Kipfstuhl, J. & Miller, H. (1994): Comparison between ice core B13 and B15.- Filchner Ronne Ice Shelf Report No 7: 29-36.

Oerter, H., Kipfstuhl, J., Determann, J., Miller, H., Wagenbach, D., Minnikin, A. & Graf, W. (1992): Evidence for basal marine ice in the Filchner-Ronne Ice Shelf.- Nature 358: 399-401.

Pickard, G.L. (1979): Descriptive physical oceanography.- Pergamon Publ., Oxford, UK. 234 pp

Pozdeev, V.S. & Kurinin, R.G. (1987): New data on ice sheet morphology, bedrock and bottom relief in the Southern Weddell Sea Basin, West Antarctica.- Antartika, Doklady Komissii 26: 66-71.

Rapp, R.P., Wang, Y.M. & Pavlis, N.K. (1991): The Ohio State 1991 Geopotential and Sea Surface Topography Harmonic Coefficient Models.- Report 410 Dept. Geod. Sc. Surv., Ohio State University, Columbus.

Reeh, N. (1982): A plasticity theory approach to the steady-state of a three-dimensional ice sheet.- J. Glaciol., 28: 431-455.

Robin, G. de Q., Doake, C.S.M., Kohnen, H., Crabtree, R.D., Jordan, S.R. & Möller, D. (1983): Regime of the Filchner-Ronne Ice Shelves, Antarctica.- Nature 302: 582-586.

Rohardt, G. (1984): Hydrographische Untersuchungen am Rand des Filchner Schelfeises.- Ber. Polarforsch. 19: 137-143.

Sanderson, T.J.O. (1979): Equilibrium profile of ice shelves.- J. Glaciol. 22: 435-460.

Sandhäger, H. (1993): Modellierung zweidimensionaler Spannungsfelder in ausgewählten Profilschnitten im Filchner-Ronne-Schelfeis (Antarktis).- Unpubl. Diploma Thesis, University of Münster, Germany. pp 161 + appendices.

Sievers, J., Doake, C.S.M, Ihde, J., Mantripp, D.R., Pozdeev, V.S., Ritter, B., Schenke, H.W., Thyssen, F. & Vaughan, D.G. (1995): Validating and improving elevation data of a satellite image map of Filchner-Ronne-Schelfeis, Antarctica, with results from ERS-1.- Ann. Glaciol. 20: 357-352.

Sievers, J., Vaughan, D.G., Bombosch, A., Doake, C.S.M., Heidrich, B., Mantripp, D.R., Pozdeev, V.S., Ritter, B., Sandhäger, H., Schenke, H.W., Swithinbank, C., Thiel, M. & Thyssen, F. (1993): Topographic Map (Satellite Image Map) 1:2 000 000 Filchner-Ronne-Schelfeis.- IfAG, Frankfurt a.M.

Smith, A.M. (1986): Ice rumples on Ronne Ice Shelf, Antarctica.- Brit. Antarct. Surv. Bull. 72: 47-52.

Smith, A.M. & Doake, C.S.M. (1994): Seabed depths at the mouth of Rutford Ice Stream, Antarctica.- Ann. Glaciol. 20: 353-356.

Stuiver, M., Denton, G.H., Hughes, T.J. & Fastook, J.L. (1981): History of the marine ice shelf in West Antarctica during the last glaciation; A working hypothesis.- In: G.H. DENTON & T.J. HUGHES (eds.), The Last Great Ice Sheets, Wiley-Interscience, New York, 319-436.

Swithinbank, C.W.M., Brunk, K. & Sievers, J. (1988): A glaciological map of Filchner-Ronne Ice Shelf, Antarctica.- Ann. Glaciol. 11: 150-155.

ten Brink, U. (1994): Tectonic subsidence and the stratigraphy of the Antarctic continental margins and intracontinental basins.- Terra Antartica 1: 255-257.

ten Brink, U. & Cooper, A.K. (1990): Factors affecting the characteristic bathymetry of Antarctic continental margins: preliminary modelling results from Prydz Bay.- ANTOSTRAT Antarctic Offshore Stratigraphy, Rep. Internat. Workshop, Asilomar Calif., 274-277.

ten Brink, U. & Schneider, C. (1994): Glacial processes affecting the stratigraphy of the Antarctic continental margin: results from modelling.- Terra Antartica 1: 435-436.

Thyssen, F., Bombosch, A. & Sandhäger, H. (1993): Elevation ice thickness and structure marks of the central part of Filchner-Ronne Ice Shelf.- Polarforsch. 62: 17-26.

Thyssen, F. (1988): Special aspects of the central part of Filchner-Ronne Ice Shelf.- Ann. Glaciol. 11: 173-179.

Thyssen, F. & Hoppe, H. (1988): Ice thickness and bedrock elevation in western Neuschwabenland and Berkner Island, Antarctica.- Ann. Glaciol. 11: 42-45.

Vaughan, D.G., Sievers, J., Doake, C.S.M., Grikurov, G., Hinze, H., Pozdeev, V.S., Sandhäger, H., Schenke, H.W., Solheim, A. & Thyssen, F. (1994): Map of subglacial and seabed topography 1: 2 000 000 Filchner-Ronne-Schelfeis/ Weddell Sea, Antarktis.- IfAG, Frankfurt a.M.